

2,2'-Biimidazole-Based Conjugated Polymers as a Novel Fluorescent Sensing Platform for Pyrophosphate Anion

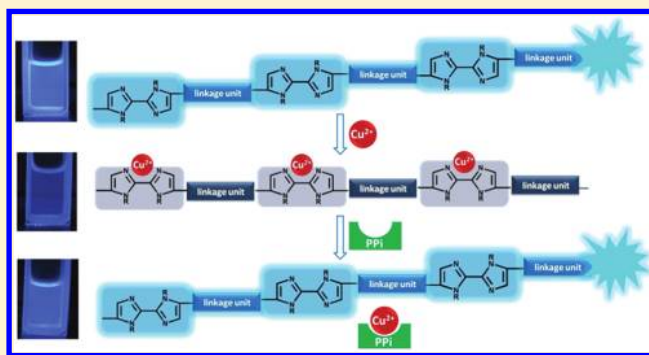
Yinyin Bao,[†] Hu Wang,[†] Qianbiao Li,[†] Bin Liu,[†] Qing Li,[†] Wei Bai,[‡] Bangkun Jin,[†] and Ruke Bai^{*,†}

[†]CAS Key Laboratory of Soft Matter Chemistry, Department of Polymer Science and Engineering, University of Science and Technology of China, Hefei 230026, P. R. China

[‡]Department of Chemistry, Louisiana State University, Baton Rouge, Louisiana 70803, United States

S Supporting Information

ABSTRACT: Three novel conjugated polymers based on 2,2'-biimidazole have been successfully designed and synthesized through the Suzuki coupling reactions, and their fluorescence sensing ability to metal ions and anions was investigated. The emission of the two polymers with hydrophilic side chains can be efficiently quenched by Cu^{2+} through a photoinduced electron transfer process. Moreover, the polymer- Cu^{2+} complexes exhibit excellent "turn on" sensing properties for detection of pyrophosphate (PPi) anion. These complex sensors possess high selectivity avoiding the interference from other anions, very fast response (less than 3 min) to PPi, and the detection limit of about 0.17 ppm. In addition, the linear detection range of PPi can be tuned conveniently by changing the amount of Cu^{2+} ions. Thus, the conjugated polymers can be used as a novel fluorescent sensing platform, and this work provides a new strategy for the development of PPi sensors.



INTRODUCTION

In recent years, conjugated polymer-based fluorescent sensors have been developed as a highly effective tool for detection of a broad range of environmental and biological analyses.¹ With "molecular wire" effect of the conjugated polymers, the detection sensitivity of the polymer sensors can be greatly enhanced because of the fast energy migration along the conjugated backbone.² Thus, conjugated polymers have more advantages over small molecules for sensing applications. Among these polymers, several N-heterocyclic aromatic units have been introduced into the backbone as molecular recognition sites for metal ions, such as bipyridyl,³ terpyridyl,⁴ and phenanthroline.⁵ After coordination with different metal ions, the polymers exhibit different fluorescence changes, such as quenching or emission red/blue shift, which can be attributed to electron density variations on the main chains, aggregation of polymer chains, or conjugation enhancement along the polymer backbone.^{3–5} However, the selectivity of polymer sensors based on N-heterocycle, especially for the bipyridyl analogue, remains unsatisfactory compared with that of the small molecule sensors.⁶ In order to improve the properties of the polymer sensors, the design and synthesis of the conjugated polymer sensors with new aromatic N-heterocycle as a receptor are still a quite important and intriguing theme.

As an important aromatic N-heterocycle, imidazole plays a significant role in biosystems and attractive chemical properties.⁷ Most recently, the conjugated polymers with imidazole or

imidazolium as the side groups have been synthesized and utilized as excellent fluorescent sensors for detection of metal ions, anions, nitric oxide, and amino acids.⁸ 2,2'-Biimidazole, the dimeric analogue of imidazole, is one of the most important derivatives of imidazole and plays a particular role in crystal engineering because of the excellent coordination ability and diverse coordination modes.⁹ In addition, 2,2'-biimidazole can be easily functionalized through various ways under mild conditions.¹⁰ However, only very few papers have been devoted to the study of the conjugated polymers containing biimidazole moiety. Yamamoto et al. prepared three 2,2'-biimidazole homopolymers by the dehalogenative polycondensation using a zerovalent nickel catalyst.^{11a} Then MacLean et al. reported conjugated polymers of 2,2'-biimidazole obtained through electrochemical polymerization.^{11b} The authors did not investigate the fluorescence properties of the polymers; they focused on the structure and chemical properties. From the literature,¹² we know that 2,2'-biimidazole has large M–N (metal–nitrogen) bond length of 4.2 Å, while 2,2'-bipyridine's M–N bond length is only 2.51 Å, which may endow 2,2'-biimidazole containing conjugated polymers with some distinguishing sensing properties.

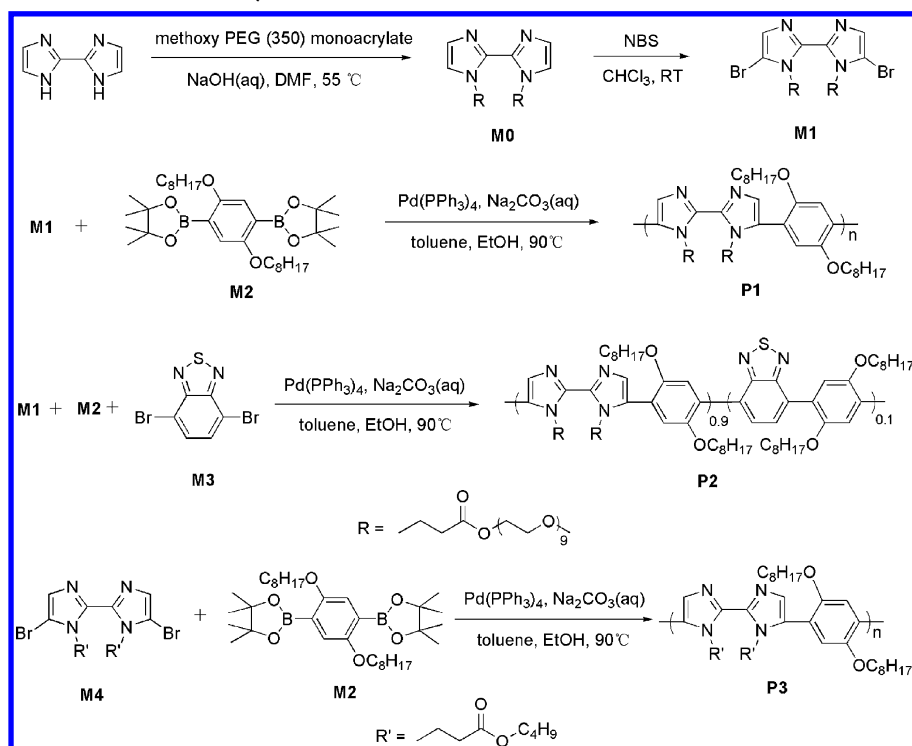
We have recently incorporated 2,2'-biimidazole into the conjugated polymer and used this kind of polymer as a new

Received: February 21, 2012

Revised: March 30, 2012

Published: April 9, 2012

Scheme 1. Synthesis of Monomers and Polymers



platform for design of different fluorescent sensors.¹³ The polymer exhibits distinctive fluorescence response to Ag^+ , which is quite different from the features of the conjugated polymers with the oligopyridyl moieties in their backbones and as well as with the imidazole moieties in their side chains. In addition, the polymer– Ag^+ complexes can be used to highly selective detection of cysteine with nanomolar detection limit. In order to further explore new sensors based on the sensing properties of the N-heterocyclic conjugated polymers, we have also designed and prepared three new conjugated polymers based on 2,2'-biimidazole (**P1**, **P2**, and **P3**, Scheme 1) and found that the polymers exhibit high quantum yields in solutions. Moreover, the fluorescence of **P1** and **P2** can be efficiently quenched by Cu^{2+} in DMF– H_2O mixed solvents. Therefore, a new sensing platform utilizing the polymer– Cu^{2+} complexes for detection of pyrophosphate (PPi) anion has been achieved. The complex sensors exhibit high selectivity and fast response to PPi with the detection limit of about 0.17 ppm, and the linear detection range of PPi can be tuned conveniently by changing the amount of Cu^{2+} ions. Herein we report the synthesis, characterization, and sensing properties of the polymers.

EXPERIMENTAL SECTION

Materials. Metal salts such as NaCl, KCl, MgCl_2 , CaCl_2 , FeCl_3 , ZnCl_2 , CdCl_2 , NiCl_2 , CuCl_2 , $\text{Mn}(\text{OAc})_2$, $\text{Pb}(\text{OAc})_2$, and AgNO_3 were purchased from Shanghai Chemical Co. and used without further purification. Et_3N and 1,4-dioxane were freshly distilled over appropriate drying agents. The reactions that required oxygen-free conditions were carried out under an argon atmosphere using standard Schlenk techniques. All the other reagents were purchased and used without further purification.

Measurements. Fluorescence spectra measurements were performed on a Shimadzu RF-5301PC spectrofluorophotometer. Absorption spectra were determined on a Pgeneral UV–vis TU-1901 spectrophotometer. ^1H and ^{13}C NMR spectra were taken on a

Bruker AVANCEII spectrometer with TMS as an internal standard and CDCl_3 as solvent. Molecular weights and molecular weight distributions were determined by GPC equipped with a Waters 1515 pump, a Waters 2414 RI detector, and Waters UV/RI detectors (set at 30 °C) using a series of three linear Styragel columns HR3, HR4, and HR6 at an oven temperature of 45 °C. Mass spectra were performed on a ProteomeX-LTQ spectrometer. FT-IR spectra were recorded on a Bruker EQUINOX55 spectrometer. All spectra were measured at room temperature (temperature controlled at 25 ± 3 °C).

Synthesis of M0. Solid 2,2'-biimidazole¹⁴ (0.67 g, 5.0 mmol) was dispersed in DMF (20 mL), and 0.5 N NaOH(aq) (1.0 mL) was added. The suspension was stirred and heated to 50 °C. A solution composed of methoxy poly(ethylene glycol) monoacrylate (5.0 g, 10.3 mmol) solubilized in DMF (10 mL) was added dropwise. After 4 h, the solution was neutralized with aqueous hydrochloric acid and the heating discontinued. The solvent was removed by rotary evaporation, and the product was chromatographed on silica gel (CH_2Cl_2 :methanol = 20:1, v/v) to give **M0** (5.5 g) as a pinkish liquid; yield: 98.7%. ^1H NMR (400 MHz, CDCl_3): δ = 7.07 (s, 2H), 7.03 (s, 2H), 4.74 (t, 4H), 4.21 (t, 4H), 3.62 (m, 68H), 3.36 (s, 6H), 2.93 (t, 4H). ^{13}C NMR (100 MHz, CDCl_3): δ = 171.3, 137.7, 127.8, 122.3, 71.9, 70.5, 68.9, 63.8, 59.0, 43.3, 35.5. MS: m/z = 1098.61.

Synthesis of M1. N-Bromosuccinimide (0.38 g, 2.13 mmol) was added to a chloroform solution (15 mL) of **M0** (1.17 g, 1.06 mmol) under vigorous stirring under air. After 2 h, the reaction mixture was neutralized with NaOH(aq), and the product was extracted with chloroform. After being washed with water, the combined organic layers were dried (Na_2SO_4) and chromatographed on silica gel (CH_2Cl_2 :methanol = 20:1, v/v) to give **M1** (2.6 g) as light yellow liquid; yield: 65.4%. ^1H NMR (400 MHz, CDCl_3): δ = 7.12 (s, 2H), 4.70 (t, 4H), 4.07 (t, 4H), 4.21 (t, 4H), 3.63 (m, 68H), 3.37 (s, 6H), 2.91 (t, 4H). ^{13}C NMR (100 MHz, CDCl_3): δ = 170.6, 138.4, 128.9, 105.8, 71.9, 70.5, 68.9, 63.9, 59.0, 42.1, 34.3. MS: m/z = 1256.43.

Synthesis of M2. 1,4-Diiodo-2,5-dioctyloxybenzene¹⁵ (1.67 g, 3.0 mmol), pinacolborane (1.32 mL, 9.0 mmol), Et_3N (2.5 mL), and $\text{PdCl}_2(\text{dppf})$ (0.05 g, 0.06 mmol) were dissolved in anhydrous 1,4-dioxane (12 mL) under an Ar atmosphere, and the solution was stirred overnight at 90 °C. After cooling to room temperature, the mixture was poured into water (50 mL) and extracted with Et_2O (3 × 20 mL).

The combined organic layers were dried (Na_2SO_4) and chromatographed on silica gel (petroleum ether:ethyl acetate = 20:1, v/v) to give **M2** (1.2 g) as a brown solid; yield: 72%. ^1H NMR (400 MHz, CDCl_3): δ = 7.08 (s, 2H), 3.93 (t, 2H), 1.74 (m, 2H), 1.47 (m, 2H), 1.34 (s, 12H), 1.30–1.24 (m, 8H), 0.88 (t, 6H). ^{13}C NMR (100 MHz, CDCl_3): δ = 157.7, 119.9, 83.4, 69.7, 31.9, 29.6, 29.5, 29.3, 26.1, 24.8, 22.7, 14.1. MS: m/z = 586.46.

Synthesis of P1. **M2** (0.23 g, 0.4 mmol), **M1** (0.5 g, 0.4 mmol), $\text{Pd}(\text{PPh}_3)_4$ (0.05 g, 0.04 mmol), and Na_2CO_3 (0.85 g, 8.0 mmol) were added to a flask under an Ar atmosphere. A solvent mixture of toluene (8 mL), water (4 mL), and ethanol (2 mL) was degassed and added to the reaction mixture. The resulting mixture was refluxed with vigorous stirring for 48 h. After cooling to room temperature, the mixture was poured into water (30 mL) and extracted with CHCl_3 (3 \times 30 mL). The collected organic layers were dried (Na_2SO_4) and purified by precipitation from ether to give **P1** (0.11 g) as a brown solid; yield: 19.6%. M_w = 8900, M_w/M_n = 1.27 (GPC, polystyrene calibration). ^1H NMR (400 MHz, CDCl_3): δ = 7.12 (br, ArH), 6.94 (br, ArH), 4.74 (br, $-\text{CH}_2-\text{O}-$), 4.13–3.89 (br, $-\text{CH}_2-\text{N}-$ and $-\text{CH}_2-\text{O}-$), 3.63–3.54 (br, $-\text{O}-\text{CH}_2\text{CH}_2-\text{O}-$), 3.36 ($-\text{O}-\text{CH}_3$), 2.76 (br, $-\text{CH}_2-\text{COO}-$), 1.69 (br, $-\text{CH}_2-$), 1.24 (br, $-\text{CH}_2-$), 0.86 (br, $-\text{CH}_3$). UV–vis (DMF, 8.0×10^{-6} mol/L): λ_{max} = 335 nm. IR (thin film), ν (cm^{-1}): 2928, 2860 (CH_2 stretching), 1737 ($\text{C}=\text{O}$ stretching), 1102 ($\text{C}-\text{O}$ stretching).

Synthesis of P2. **P2** was prepared by reaction of **M2** (0.17 g, 0.3 mmol), **M1** (0.34 g, 0.27 mmol), and 4,7-dibromo-2,1,3-benzothiadiazole (0.009 g, 0.03 mmol) using the same procedure as **P1**. The yield was 23% of **P2** (0.09 g) as a brown solid. M_w = 5200, M_w/M_n = 1.28 (GPC, polystyrene calibration). ^1H NMR (400 MHz, CDCl_3): δ = 7.47–6.93 (br, ArH), 4.75 (br, $-\text{CH}_2-\text{O}-$), 4.15–3.93 (br, $-\text{CH}_2-\text{N}-$ and $-\text{CH}_2-\text{O}-$), 3.63–3.54 (br, $-\text{O}-\text{CH}_2\text{CH}_2-\text{O}-$), 3.37 ($-\text{O}-\text{CH}_3$), 2.75 (br, $-\text{CH}_2-\text{COO}-$), 1.81–1.45 (br, $-\text{CH}_2-$), 1.23 (br, $-\text{CH}_2-$), 0.86 (br, $-\text{CH}_3$). UV–vis (DMF, 8.0×10^{-6} mol/L): λ_{max} = 326 nm. IR (thin film), ν (cm^{-1}): 2926, 2855 (CH_2 stretching), 1735 ($\text{C}=\text{O}$ stretching), 1100 ($\text{C}-\text{O}$ stretching).

Synthesis of P3. **P3** was prepared by reaction of **M2** (0.17 g, 0.3 mmol) and **M4**¹³ (0.16 g, 0.3 mmol) using the same procedure as **P1**, except that the polymer was purified by precipitation from methanol to give a slightly gray solid (0.09 g); yield: 45%. M_w = 12 000, M_w/M_n = 1.40 (GPC, polystyrene calibration). ^1H NMR (400 MHz, CDCl_3): δ = 7.14 (ArH), 6.95 (ArH), 4.78 (br, $-\text{CH}_2-\text{N}-$), 4.11–3.93 (br, $-\text{CH}_2-\text{O}-$), 2.76 (br, $-\text{CH}_2-\text{COO}-$), 1.71–1.53 (br, $-\text{CH}_2-$), 1.34–1.25 (br, $-\text{CH}_2-$), 0.91–0.85 (br, $-\text{OCHH}_3$). UV–vis (DMF, 8.0×10^{-6} mol/L): λ_{max} = 336 nm. IR (thin film), ν (cm^{-1}): 2965, 2904 (CH_2 stretching), 1735 ($\text{C}=\text{O}$ stretching), 1100 ($\text{C}-\text{O}$ stretching).

Fluorometric Analysis. The stock solutions of **P1**, **P2**, and **P3** were prepared by dissolving the polymers in DMF (1.0×10^{-3} M) and were diluted as required before use. The cation stock solutions were prepared by dissolving the metal salts in deionized water with a concentration of 0.01 M. The stock solutions of F^- , Cl^- , Br^- , I^- , NO_3^- , HSO_4^- , AcO^- , HCO_3^- , CO_3^{2-} , H_2PO_4^- , HPO_4^{2-} , PO_4^{3-} , and $\text{P}_2\text{O}_7^{2-}$ were prepared in deionized water with a concentration of 0.01 M. A solution of polymer (2.0 mL) was placed in a quartz cell (10.0 mm width), and the fluorescence spectrum was recorded. The sum volume of each ion solution introduced to the test solution was no more than 50 μL , and the changes of the fluorescence intensity were recorded at room temperature (λ_{ex} = 338 nm). The quantum yields of the polymers were determined according to the equation

$$\Phi_u = \Phi_s \frac{F_u A_s n_u^2}{F_s A_u n_s^2}$$

where Φ is quantum yield, F is integrated area under the corrected emission spectra, A is absorbance at the excitation wavelength, n is the refractive index of the solution, and the subscripts u and s refer to the unknown and the standard, respectively. Quinine bisulfate in 0.05 M H_2SO_4 solution was used as the standard, which has a quantum yield of 0.55.

RESULTS AND DISCUSSION

Design and Synthesis. The polymers **P1**, **P2**, and **P3** were synthesized by Suzuki condensation, and the synthetic routes are illustrated in Scheme 1. 2,2'-Biimidazole was prepared according to the published procedure¹⁴ and then was reacted with methoxy poly(ethylene glycol) monoacrylate through Michael addition reaction to form **M0**. Subsequently, **M0** was brominated with *N*-bromosuccinimide (NBS) at room temperature, resulting 5,5'-dibromo-*N,N'*-di(methoxy poly(ethylene glycol) monoacrylate propionato)-2,2'-biimidazole (**M1**) as a hydrophilic monomer. A hydrophobic monomer 5,5'-dibromo-*N,N'*-di(*n*-butylpropionato)-2,2'-biimidazole (**M4**) was synthesized by a similar method.¹³ Monomer **M2** (1,4-bis(4,4,5,5-tetramethyl-1,3,2-dioxaborolan-2-yl)-2,5-dioctyloxyphenylene) was synthesized from 1,4-diiodo-2,5-dioctyloxybenzene¹⁵ through borylation reaction catalyzed by $\text{PdCl}_2(\text{dppf})$,¹⁶ and monomer **M3** (4,7-dibromo-2,1,3-benzothiadiazole) was prepared according to the literature procedures.¹⁷ **P1** was conveniently formed via Suzuki coupling reaction between **M1** and **M2** catalyzed by the $\text{Pd}(\text{PPh}_4)_3$, and **P3** was obtained in a similar approach with **M4** and **M2**. **P2** was synthesized utilizing 1.0 equiv of **M2**, 0.9 equiv of **M1**, and 0.1 equiv of **M3**. **P1** and **P2** were purified by precipitation from ether and collected as brown solids, while **P3** was obtained by precipitation from methanol as a slightly gray solid. It is worthy to point out that 2,2'-biimidazole-based monomers were efficiently synthesized under mild conditions, which makes the 2,2'-biimidazole containing polymers more accessible compared with the other N-heterocycle-based main chain conjugated polymers. Utilizing the 2,2'-biimidazole-based monomers, different kinds of conjugated polymers can be prepared conveniently, resulting a new series of fluorescence sensing molecules.

Characterization of Polymers. The purified polymers were characterized by ^1H NMR, FT-IR, UV–vis, and GPC analysis (see Experimental Section and Supporting Information for detailed analysis data). In the ^1H NMR spectra of the polymers **P1**, **P2**, and **P3** (Figure 1 and Figures S34 and S35),

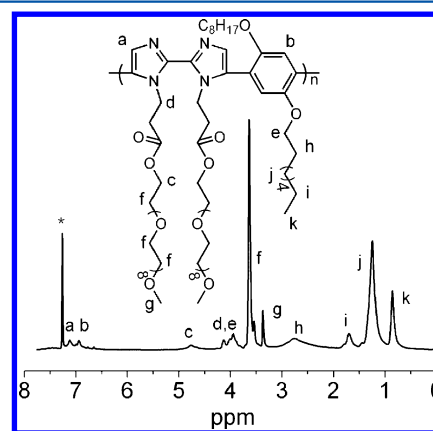


Figure 1. ^1H NMR spectra of **P1** in chloroform-*d*. The solvent peak was marked with asterisks.

the chemical shifts are consistent with the proposed structure of the polymers as demonstrated in Scheme 1. Take **P1** for example; as shown in Figure 1, the two peaks at about 7.12 and 6.94 ppm in the downfield can be ascribed to the aromatic protons of biimidazole unit and benzene unit, respectively, indicating **M1** and **M2** have been successfully copolymerized

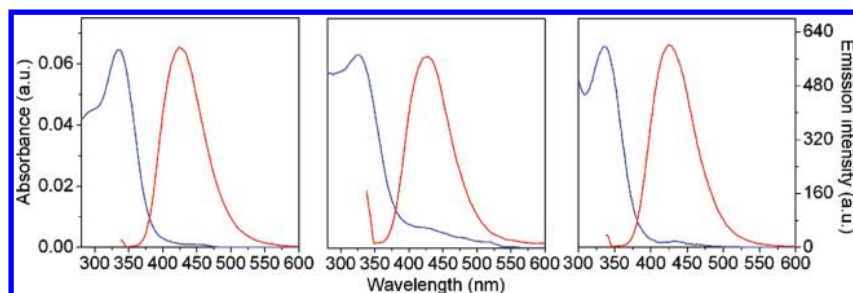


Figure 2. UV-vis absorption (blue line) and fluorescence spectra (red line) of **P1** (left), **P2** (middle), and **P3** (right) in DMF. $[P1] = [P2] = [P3] = 8.0 \times 10^{-6}$ M. $\lambda_{\text{ex}} = 338$ nm.

through Suzuki condensation. And the existence of the ether side chains and octyl side chains can be confirmed by the peaks at 3.36 and 0.86, which can also be supported by the bands at 2965 and 2904 cm^{-1} of C-H vibration stretching, 1737 cm^{-1} of C=O stretching, and 1102 cm^{-1} of C-O stretching in the FT-IR spectrum of **P1** (Figure S36).

The three polymers readily dissolve in common organic solvents, such as toluene, CH_2Cl_2 , THF, and DMF, because of the flexible alkyl or ether side chains. The molecular weights (M_n) and polydispersity index (PDI) of the polymers were determined by gel permeation chromatography (GPC) with polystyrene as the reference standard (Table S1). The molecular weights of the polymers are relatively low, which may be because the polymerization reactivity of the 2,2'-biimidazole-based monomers is not very high. Even so, the molecular weights are high enough for the polymers to have good sensing properties, and a similar phenomenon can be seen in the previous reports³⁻⁵ on polycondensation of N-heterocycle-based monomers. The UV-vis absorption spectra of polymers are shown in Figure 2, **P1**, **P2**, and **P3** have similar maximum absorption wavelengths around 330 nm in DMF because of the similar conjugated backbone. But **P2** has stronger absorption from 400 to 550 nm, which can be attributed to the alkoxybenzene-benzothiadiazole units. All the evidence indicates that the designed polymers have been successfully prepared.

Fluorescence Properties and Ion Recognition. The emission spectra of **P1** and **P2** were measured in various organic solvents at room temperature (Figures S1 and S2). It can be seen that the two polymers exhibit highest emission intensity in DMF, so it was chosen as the main solvent to investigate the fluorescence properties of the polymers. The results show that all the three polymers exhibit a strong blue fluorescence with a maximum around 425 nm in DMF because of the conjugated polymer backbone. However, in the presence of alkoxybenzene-benzothiadiazole units, **P2** shows a little broader emission peak. Simultaneously, a Förster resonance energy transfer (FRET) process may exist in **P2** because the weak absorption peak of the alkoxybenzene-benzothiadiazole unit can be found to overlap with the emission peak of the alkoxybenzene-biimidazole unit. The orange emission peak around 550 nm can be observed more obviously in the solution of THF, dioxane, and toluene than in DMF (Figure S2), and a similar phenomenon has also been observed in our previous report.¹³ The fluorescence quantum yields of **P1**, **P2**, and **P3** in DMF were determined to be 0.22, 0.10, and 0.41, respectively. In order to examine the properties of these polymers in aqueous solution, the fluorescence spectra of the three polymers in DMF-H₂O mixed solvents were studied. As shown in Figures S3-S6, the emission intensity of the polymers

decreases along with increasing the water content; this can be attributed to the chain aggregation-induced fluorescence quenching. Note that **P3** shows much faster quenching rate than the other two polymers (Figure S7). This phenomenon indicates that both **P1** and **P2** with hydrophilic side chains can be better dispersed in DMF-H₂O mixed solvents. Thus, **P1** and **P2** are more suitable for fluorescence sensing application in aqueous solution compared with **P3**. Moreover, as shown in Figure S5, the fluorescence intensity ratios $F_{550 \text{ nm}}/F_{423 \text{ nm}}$ of **P2** increases along with raising the water content, and after the water content reaches 90% the emission peak at 423 nm disappeared, resulting a single peak at 550 nm (Figure S4). This result can be largely ascribed to the fact that the FRET effect existing in **P2** system is distinctly enhanced because of water-induced chain aggregation.¹³

Since the polymers **P1** and **P2** show high fluorescence quantum yield (Table S1) and good dispersion in DMF-H₂O (4:1, v/v), we chose the mixed solvent as the detection media, and HEPES was used as the buffer agent. The ion responsive properties of **P1** were studied by fluorescence spectroscopy in DMF-HEPES (pH = 7.4, v/v = 4:1) at a concentration of 8.0×10^{-6} M. The experimental result displays that the fluorescence of **P1** can be efficiently quenched by Cu^{2+} ions. As shown in Figure 3, upon the addition of Cu^{2+} , the emission

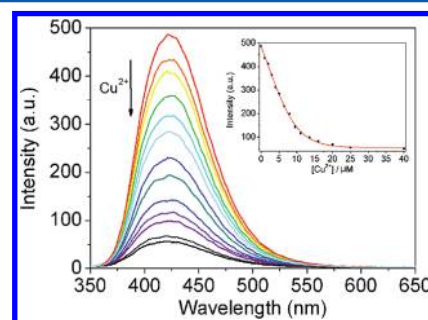


Figure 3. Fluorescence spectra of **P1** upon the titration of Cu^{2+} in DMF-HEPES (pH = 7.4, v/v = 4:1). Inset: fluorescence intensity of **P1** as a function of Cu^{2+} concentration. $\lambda_{\text{ex}} = 338$ nm. $[P1] = 8.0 \times 10^{-6}$ M.

peaks at 423 nm gradually decrease along with increasing the Cu^{2+} concentration. The intensity exhibits a good linear response to a Cu^{2+} concentration change from 0 to 1.0 equiv, and after adding 2.5 equiv of Cu^{2+} , 90% of the fluorescence has been quenched. The quenching efficiency can be described by the Stern-Volmer equation, $I_0/I = K_{\text{sv}}[A] + 1$, which related to the fluorescence intensity, I , at different concentrations of analyte quencher, $[A]$, where I_0 is the intensity at $[A] = 0$ and K_{sv} is the Stern-Volmer constant. According to the

fluorescence titration of **P1** in DMF aqueous solution with Cu^{2+} , K_{sv} of the system was determined to be $3.3 \times 10^5 \text{ M}^{-1}$ (Figure S8). When the quantum yield of **P1** changed from 0.13 to 0.02 upon interaction with Cu^{2+} , the obvious fluorescence changes could be observed by the naked eye under a UV lamp. For comparison's sake, the Cu^{2+} response properties of **P3** were also studied (Figures S13–S15). However, the Stern–Volmer quenching constant K_{sv} of **P3**– Cu^{2+} was calculated to be only $2.8 \times 10^3 \text{ M}^{-1}$ (Figure S15), which is much lower than that of **P1**– Cu^{2+} . And after addition of 20.0 equiv of Cu^{2+} , only 30% of the fluorescence can be quenched. This result indicates that **P1** has much stronger coordination ability with Cu^{2+} than **P3** in DMF– H_2O mixed solvent, which implies that the hydrophilic side chains can promote the interaction between the polymer and Cu^{2+} ions in aqueous solution. Thus, the reasonable design of side chains is important to construct conjugated polymer-based fluorescent sensors.

In general, there are two possibilities that metal ions cause an obvious fluorescence quenching phenomenon of conjugated polymer: one is electron transfer interactions between the polymer backbone and metal ions, and the other is interpolymer aggregation induced by coordination. To further clarify the mechanism, we investigated the fluorescence response properties of **P2** to Cu^{2+} in aqueous DMF solution. If the fluorescence quenching is induced by chain aggregation, after adding enough Cu^{2+} ions the FRET enhancement similar to the phenomenon caused by water (Figure S4) should be observed, leading to a large change of intensity ratios $F_{550 \text{ nm}}/F_{423 \text{ nm}}$. However, upon interaction with Cu^{2+} , the intensity ratios $F_{550 \text{ nm}}/F_{423 \text{ nm}}$ exhibits only a slight increment, and no obvious emission peak at 550 nm was actually observed in the **P2** system (Figures S9 and S10), which means aggregation of polymer chains is not the principal contributor to the quenching phenomenon in the system. Thus, we may reasonably conclude that the emission quenching of the polymers is mainly due to electron transfer interactions between the polymer backbone and Cu^{2+} ions, which was also reported in the previous paper.^{8c} In addition, this work provides an efficient method to investigate the sensing mechanism of conjugated polymers to metal ions, which was not reported in the literature of other N-heterocycle-based polymer sensors.^{3–5,8} At the same time, the Stern–Volmer constant K_{sv} of **P2**– Cu^{2+} was calculated to be $2.6 \times 10^5 \text{ M}^{-1}$ (Figure S12), which is of the same order of magnitude as, but a little lower than, that of the **P1**– Cu^{2+} system. This result shows that the fluorescence of **P2** can also be efficiently quenched by Cu^{2+} , and the lower Stern–Volmer constant compared to that of **P1**– Cu^{2+} system may be attributed to the lower molecular weight, resulting in a slightly weaker “molecular wire” effect. Thus, the electron transfer interactions between the polymers and Cu^{2+} can be tuned by changing the molecular weight of the polymer. Therefore, the reasonable design of the backbone is critical to develop efficient conjugated polymer-based fluorescent sensors. In addition, the coordination reaction of **P1** and **P2** with Cu^{2+} has been confirmed by the UV–vis titration experiment (Figures S16 and S17).

As shown in Figures S18–S21, compared with other metal ions, Cu^{2+} ion shows the strongest quenching ability to the polymers. It is well-known that pyrophosphate (PPi) anion has strong interaction with Cu^{2+} ;¹⁸ thus, we attempted to use these polymer– Cu^{2+} complexes as new sensors for detection of PPi. PPi is a biologically important target because it is the product of ATP hydrolysis under cellular conditions.¹⁹ There are many

papers published on the study of PPI fluorescent sensors based on the metal ion complexes²⁰ and hydrogen-bond or ionic bond interaction.²¹ However, only very few PPI sensors based on conjugated polymers have been reported.²² Herein we prepared the Cu^{2+} complexes of the conjugated polymers containing 2,2'-biimidazole moieties *in situ* by mixing **P1** and **P2** with Cu^{2+} salt in aqueous DMF, respectively, and studied their sensing properties for PPI. The results indicate that the emission spectra of the complexes exhibit remarkable changes upon interaction with PPI. As shown in Figure 4, the emission

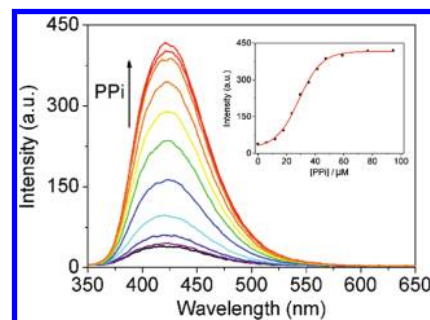


Figure 4. Fluorescence spectra of **P1**– Cu^{2+} complex upon the titration of PPI in DMF–HEPES (pH = 7.4, v/v = 4:1). Inset: fluorescence intensity of **P1**– Cu^{2+} complex as a function of PPI concentration. λ_{ex} = 338 nm. $[\text{P1}] = 8.0 \times 10^{-6} \text{ M}$. $[\text{Cu}^{2+}] = 2.0 \times 10^{-5} \text{ M}$.

peak of **P1**– Cu^{2+} ($[\text{P1}] = 8.0 \times 10^{-6} \text{ M}$, $[\text{Cu}^{2+}] = 2.0 \times 10^{-5} \text{ M}$) gradually increases upon addition of different amount of PPI anions, and the intensity at 423 nm exhibits a good linear change with a PPI concentration increasing from 1.0×10^{-5} to $4.8 \times 10^{-5} \text{ M}$. Moreover, when utilizing $1.0 \times 10^{-5} \text{ M}$ Cu^{2+} and $8.0 \times 10^{-6} \text{ M}$ **P1** as the sensing ensemble, the emission intensity changes linearly with the concentration of PPI from 5.0×10^{-6} to $1.6 \times 10^{-5} \text{ M}$ (Figure 5). Thus, the linear change

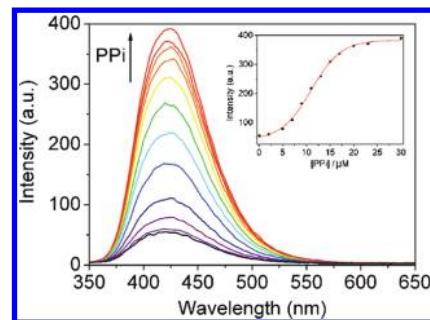
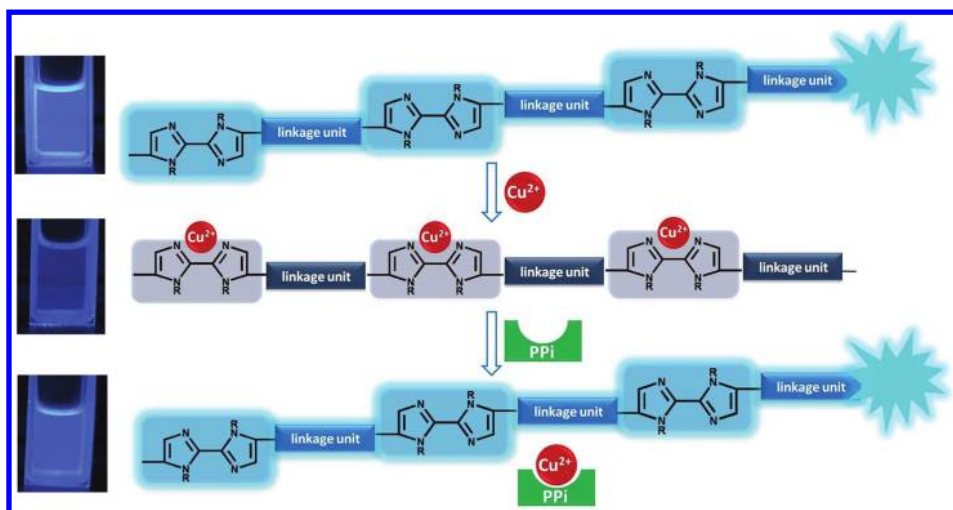


Figure 5. Fluorescence spectra of **P1**– Cu^{2+} complex upon the titration of PPI in DMF–HEPES (pH = 7.4, v/v = 4:1). Inset: fluorescence intensity of **P1**– Cu^{2+} complex as a function of PPI concentration. λ_{ex} = 338 nm. $[\text{P1}] = 8.0 \times 10^{-6} \text{ M}$. $[\text{Cu}^{2+}] = 1.0 \times 10^{-5} \text{ M}$.

range of PPI can be tuned by varying the amount of Cu^{2+} ions. After adding 5.0 equiv of PPI, a 9-fold emission enhancement can be obtained, and the fluorescence changes under a UV lamp can be distinctly observed by the naked eye (Chart 1). From the fluorescence titration experiment, the detection limit of PPI was estimated to be less than $1.0 \times 10^{-6} \text{ M}$, about 0.17 ppm. Similar to **P1**, **P2** also shows good turn-on sensing properties for PPI in the presence of Cu^{2+} ions (Figures S22–S25). As shown in Figures S23 and S25, the linear range 1.0×10^{-5} – $3.6 \times 10^{-5} \text{ M}$ can be changed into 5.0×10^{-6} – $2.4 \times 10^{-5} \text{ M}$ by varying the concentration of Cu^{2+} from 2.0×10^{-5} to 1.0

Chart 1. Schematic Representation of PPI Sensors Based on the Fluorescence “On–Off–On” of 2,2'-Biimidazole Containing Conjugated Polymers



$\times 10^{-5}$ M. The sensing process is consistent with the displacement approach reported in the previous report^{18,20} utilizing metal ion complexes, the fluorescence of the polymers can be recovered once the Cu^{2+} ions are removed by PPI, and the possible sensing mechanism is illustrated in Chart 1. These sensors are based on the interaction of PPI with Cu^{2+} ions coordinated to the biimidazole group on polymer backbone, while the other polymer PPI sensors²² rely on the interaction of PPI with Cu^{2+} on the polymer side chains or directly with the polymers.

The response time is very important for a sensor; therefore, the effect of the interaction time on the fluorescence emission of the system has been examined, and the results are shown in Figure 6. It can be seen that the emission intensity of P1-Cu^{2+}

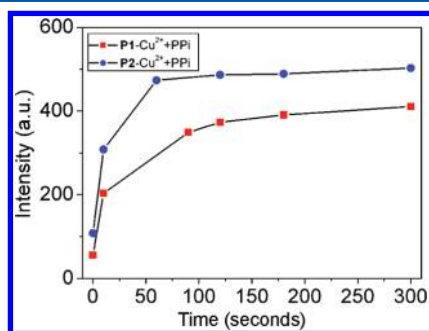


Figure 6. Effect of reaction time on the fluorescence intensity of P1-Cu^{2+} and P2-Cu^{2+} by PPI ions in DMF-HEPES (pH = 7.4, v/v = 4:1). $\lambda_{\text{ex}} = 338$ nm. $[\text{P1}] = [\text{P2}] = 8.0 \times 10^{-6}$ M. $[\text{Cu}^{2+}] = 2.0 \times 10^{-5}$ M. $[\text{PPI}] = 4.0 \times 10^{-5}$ M.

reaches to its saturation value in just 3 min due to the strong interaction of Cu^{2+} ions with the PPI anions. On the other hand, the response time of P2-Cu^{2+} to PPI is only 1 min, much shorter than that of P1-Cu^{2+} . The reason is that **P2** has weaker binding ability to Cu^{2+} than **P1** due to the lower molecular weight, which can be deduced from the Stern–Volmer constants. Since P2-Cu^{2+} complex possesses a faster response, it can be used as an excellent sensor for rapid detection of PPI. We can conclude that the fluorescence sensing properties of conjugated polymer based fluorescent sensors can be efficiently optimized through the reasonable structure modification.

To determine the selectivity of the PPI-sensing systems, the fluorescence responses of P1-Cu^{2+} and P2-Cu^{2+} complexes were further examined with 13 different anions including monovalent anions (F^- , Cl^- , Br^- , I^- , NO_3^- , HSO_4^- , AcO^- , HCO_3^- , H_2PO_4^-), divalent anions (CO_3^{2-} , HPO_4^{2-}), and trivalent ion PO_4^{3-} . As shown in Figure 7 and Figures S26 and

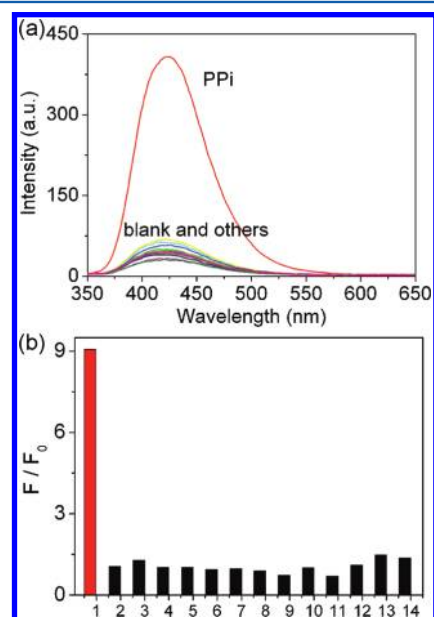


Figure 7. (a) Fluorescence spectra of P1-Cu^{2+} complex and (b) intensity ratios F/F_0 of P1-Cu^{2+} complex in the presence of 4.0×10^{-5} M PPI and 8.0×10^{-5} M various anions in DMF-HEPES (pH = 7.4, v/v = 4:1). $\lambda_{\text{ex}} = 338$ nm. $[\text{P1}] = 8.0 \times 10^{-6}$ M. $[\text{Cu}^{2+}] = 2.0 \times 10^{-5}$ M. 1, PPI; 2, F^- ; 3, Cl^- ; 4, Br^- ; 5, I^- ; 6, NO_3^- ; 7, HSO_4^- ; 8, ClO_4^- ; 9, AcO^- ; 10, HCO_3^- ; 11, CO_3^{2-} ; 12, H_2PO_4^- ; 13, HPO_4^{2-} ; 14, PO_4^{3-} .

S27, the experiment results indicate that all of the other anions exhibit weak binding affinities to Cu^{2+} ion and lead to negligible changes in the fluorescence properties of the complexes. Therefore, PPI can be easily differentiated from the other anions, especially from PO_4^{3-} , by the emission intensity. This

result indicates that the novel polymer complexes exhibit a high selectivity for detecting PPI.

CONCLUSIONS

In summary, we have successfully designed and synthesized three novel conjugated polymers based on 2,2'-biimidazole through the Suzuki coupling reaction and also investigated their ability to sense metal ions and anions. The fluorescence of the two polymers with hydrophilic side chains can be efficiently quenched by Cu^{2+} ions through a photoinduced electron transfer process. Based on the unique interaction of Cu^{2+} with the polymers, the two conjugated polymer- Cu^{2+} complexes have been demonstrated to be potential "turn on" fluorescent sensors for detection of pyrophosphate anion. The sensors possess high sensitivity to PPI with the detection limit of about 0.17 ppm and excellent selectivity avoiding the interference from other anions. And the linear detection range of PPI can be tuned conveniently by changing the amount of Cu^{2+} ions. Since the sensors display very fast response (less than 3 min), it provides a rapid and efficient approach for the detection of PPI. The experiment results show that the fluorescence sensing properties of the polymers can be efficiently optimized through the reasonable structure modification. In addition, the facile synthesis of the 2,2'-biimidazole-based conjugated polymers under mild conditions makes the sensors more accessible compared with the other N-heterocycle-based conjugated polymers. To the best of our knowledge, this is the first example utilizing the 2,2'-biimidazole-based conjugated polymers to detect PPI, and this work provides not only a new strategy for the development of PPI sensors but also a novel platform to further design different fluorescent sensors for other analytes.

ASSOCIATED CONTENT

Supporting Information

^1H NMR of monomers; ^{13}C NMR of monomers; ^1H NMR of P2 and P3; optical data of polymers P1 and P2 in various organic solvents; optical data of polymers P1–P3 in aqueous DMF solution with different water contents; optical data of polymers P1 and P2 in the presence of various metal ions in DMF–HEPES (pH = 7.4, v/v = 4:1); UV–vis absorption and fluorescence titration experiment data of P1–P3 to Cu^{2+} and PPI; selectivity of P2– Cu^{2+} to PPI; FT-IR spectra of P1–P3. This material is available free of charge via the Internet at <http://pubs.acs.org>.

AUTHOR INFORMATION

Corresponding Author

*Tel 86-551-3600722; Fax 86-551-3631760; e-mail bairk@ustc.edu.cn.

Notes

The authors declare no competing financial interest.

ACKNOWLEDGMENTS

The financial support from National Natural Science Foundation of China (No. 20974104 and No. 21074120) and Ministry of Science and Technology of China (No. 2007CB936401) is gratefully acknowledged.

REFERENCES

(1) (a) Toal, S. J.; Trogler, W. C. *J. Mater. Chem.* **2006**, *16*, 2871–2883. (b) Feng, F.; He, F.; An, L.; Wang, S.; Li, Y.; Zhu, D. *Adv. Mater.*

2008, *20*, 2959–2964. (c) Fan, L.-J.; Zhang, Y.; Murphy, C. B.; Angell, S. E.; Parkera, M. F.L.; Flynn, B. R.; Jones, W. E., Jr. *Coord. Chem. Rev.* **2009**, *253*, 410–422. (d) Liu, Y.; Ogawa, K.; Schanze, K. S. *J. Photochem. Photobiol., C* **2009**, *10*, 173–190. (e) Feng, X.; Liu, L.; Wang, S.; Zhu, D. *Chem. Soc. Rev.* **2010**, *39*, 2411–2419. (f) Li, K.; Liu, B. *Polym. Chem.* **2010**, *1*, 252–259. (g) Duarte, A.; Pu, K.-Y.; Liu, B.; Bazan, G. C. *Chem. Mater.* **2011**, *23*, 501–515. (h) Rostami, A.; Taylor, M. S. *Macromol. Rapid Commun.* **2012**, *33*, 21–34.

(2) (a) Swager, T. M. *Acc. Chem. Res.* **1998**, *31*, 201–207. (b) McQuade, D. T.; Pullen, A. E.; Swager, T. M. *Chem. Rev.* **2000**, *100*, 2537–2574. (c) Thomas, S. W., III; Joly, G. D.; Swager, T. M. *Chem. Rev.* **2007**, *107*, 1339–1386.

(3) (a) Wang, B.; Wasielewski, M. R. *J. Am. Chem. Soc.* **1997**, *119*, 12–21. (b) Chen, L. X.; Jalger, W. J. H.; Gosztola, D. J.; Niemczyk, M. P.; Wasielewski, M. R. *J. Phys. Chem. B* **2000**, *104*, 1950–1960. (c) Liu, B.; Yu, W.-L.; Pei, J.; Liu, S.-Y.; Lai, Y.-H.; Huang, W. *Macromolecules* **2001**, *34*, 7932–7940. (d) Smith, R. C.; Tennyson, A. G.; Lim, M. H.; Lippard, S. J. *Org. Lett.* **2005**, *7*, 3573–3575. (f) Liu, Y.; Zhang, S.; Miao, Q.; Zheng, L.; Zong, L.; Cheng, Y. *Macromolecules* **2007**, *40*, 4839–4847. (g) He, S.; Iacono, S. T.; Budy, S. M.; Dennis, A. E.; Smith, D. W.; Smith, R. C. *J. Mater. Chem.* **2008**, *18*, 1970–1976. (h) Kaes, C.; Katz, A.; Hosseini, M. W. *Chem. Rev.* **2000**, *100*, 3553–3590.

(4) (a) Kimura, M.; Horai, T.; Hanabusa, K.; Shirai, H. *Adv. Mater.* **1998**, *10*, 459–462. (b) Zhang, Y.; Murphy, C. B.; Jones, W. E. *Macromolecules* **2002**, *35*, 630–636.

(5) (a) Yasuda, T.; Yamaguchi, I.; Yamamoto, T. *Adv. Mater.* **2003**, *15*, 293–296. (b) Yasuda, T.; Yamamoto, T. *Macromolecules* **2003**, *36*, 7513–7519. (c) Zhang, M.; Lu, P.; Ma, Y.; Shen, J. *J. Phys. Chem. B* **2003**, *107*, 6535–6538. (d) Liu, X.; Zhou, X.; Shu, X.; Zhu, J. *Macromolecules* **2009**, *42*, 7634–7637.

(6) (a) Ajayaghosh, A.; Carol, P.; Sreejith, S. *J. Am. Chem. Soc.* **2005**, *127*, 14962–14963. (b) Dennis, A. E.; Smith, R. C. *Chem. Commun.* **2007**, 4641–4643. (c) Sreejith, S.; Divya, K. P.; Ajayaghosh, A. *Chem. Commun.* **2008**, 2903–2905. (d) Cockrell, G. M.; Zhang, G.; VanDerveer, D. G.; Thummel, R. P.; Hancock, R. D. *J. Am. Chem. Soc.* **2008**, *130*, 1420–1430.

(7) Fox, S. W. *Chem. Rev.* **1943**, *32*, 47–71.

(8) (a) Ho, H. A.; Leclerc, M. *J. Am. Chem. Soc.* **2003**, *125*, 4412–4413. (b) Zhou, X.-H.; Yan, J.-C.; Pei, J. *Macromolecules* **2004**, *37*, 7078–7080. (c) Xing, C.; Yu, M.; Wang, S.; Shi, Z.; Li, Y.; Zhu, D. *Macromol. Rapid Commun.* **2007**, *28*, 241–245. (d) Zeng, Q.; Cai, P.; Li, Z.; Qina, J.; Tang, B. Z. *Chem. Commun.* **2008**, 1094–1096. (e) Li, Z.; Lou, X.; Yu, H.; Li, Z.; Qin, J. *Macromolecules* **2008**, *41*, 7433–7439. (f) Zeng, Q.; Jim, C. K. W.; Lam, J. W. Y.; Dong, Y.; Li, Z.; Qin, J.; Tang, B. Z. *Macromol. Rapid Commun.* **2009**, *30*, 170–175. (g) Salinas-Castillo, A.; Camprubi-Robles, M.; Mallavia, R. *Chem. Commun.* **2010**, *46*, 1263–1265.

(9) Tadokoro, M.; Nakasuji, K. *Coord. Chem. Rev.* **2000**, *198*, 205–218.

(10) (a) Barnett, M.; Secondo, P.; Collier, H. *J. Heterocycl. Chem.* **1996**, *33*, 1363. (b) Sánchez-García, D.; Borrós, S.; Nonell, S.; Borrell, J. I.; Colominas, C.; Teixidó, J. *J. Heterocycl. Chem.* **2002**, *39*, 733. (c) Matthews, D. P.; McCarthy, J. R.; Whitten, J. P.; Kastner, P. R.; Barney, C. L.; Marshall, F. N.; Ertel, M. A.; Burkhardt, T.; Shea, P. J.; Kariyat, T. *J. Med. Chem.* **1990**, *33*, 317–327.

(11) (a) Yamamoto, T.; Uemura, T.; Tanimoto, A.; Sasaki, S. *Macromolecules* **2003**, *36*, 1047–1053. (b) Walker, D. T.; Douglas, C. D.; MacLean, B. J. *Can. J. Chem.* **2009**, *87*, 729–737.

(12) Buist, D.; Williams, N. J.; Reibenspies, J. H.; Hancock, R. D. *Inorg. Chem.* **2010**, *49*, 5033–5039.

(13) Bao, Y.; Li, Q.; Liu, B.; Du, F.; Tian, J.; Wang, H.; Wang, Y.; Bai, R. *Chem. Commun.* **2012**, *48*, 118–120.

(14) Fieselmann, B. F.; Hendrickson, D. N.; Stucky, G. D. *Inorg. Chem.* **1978**, *17*, 2078–2084.

(15) Weder, C.; Wrighton, M. S. *Macromolecules* **1996**, *29*, 5157–5165.

(16) (a) Murata, M.; Watanabe, S.; Masuda, Y. *J. Org. Chem.* **1997**, *62*, 6458–6459. (b) Bao, Y.; Liu, B.; Wang, H.; Du, F.; Bai, R. *Anal. Methods* **2011**, *3*, 1274–1276.

(17) Neto, B. A. D.; Lopes, A. S.; Ebeling, G.; Gonçalves, R. S.; Costa, V. E. U.; Quina, F. H.; Dupont, J. *Tetrahedron* **2005**, *61*, 10975–10982.

(18) (a) Kim, S. K.; Lee, D. H.; Hong, J.-I.; Yoon, J. *Acc. Chem. Res.* **2009**, *42*, 23–31. (b) Fabbri, L.; Marcotte, N.; Stomeo, F.; Taglietti, A. *Angew. Chem., Int. Ed.* **2002**, *41*, 3811–3814. (c) Huang, X.; Guo, Z.; Zhu, W.; Xie, Y.; Tian, H. *Chem. Commun.* **2008**, 5143–5145. (d) Guo, Z.; Zhu, W.; Tian, H. *Macromolecules* **2010**, *43*, 739–744. (e) Kim, M. J.; Swamy, K. M. K.; Lee, K. M.; Jagdale, A. R.; Kim, Y.; Kim, S.-J.; Yoon, K. H.; Yoon, J. *Chem. Commun.* **2009**, 7215–7217. (f) Zhang, J. F.; Park, M.; Ren, W. X.; Kim, Y.; Kim, S. J.; Jung, J. H.; Kim, J. S. *Chem. Commun.* **2011**, *47*, 3568–3570.

(19) Mathews, C. P.; van Hold, K. E. *Biochemistry*; The Benjamin/Cummings Publishing Co., Inc.: Redwood City, CA, 1990.

(20) (a) Mizukami, S.; Nagano, T.; Urano, Y.; Odani, A.; Kikuchi, K. *J. Am. Chem. Soc.* **2002**, *124*, 3920–3925. (b) Lee, D. H.; Kim, S. Y.; Hong, J.-I. *Angew. Chem., Int. Ed.* **2004**, *43*, 4777–4780. (c) Aoki, S.; Kagata, D.; Shiro, M.; Takeda, K.; Kimura, E. *J. Am. Chem. Soc.* **2004**, *126*, 13377–13390. (d) Jang, Y. J.; Jun, E. J.; Lee, Y. J.; Kim, Y. S.; Kim, J. S.; Yoon, J. *J. Org. Chem.* **2005**, *70*, 9603–9606. (e) Lee, H. N.; Xu, Z.; Kim, S. K.; Swamy, K. M. K.; Kim, Y.; Kim, S.-J.; Yoon, J. *J. Am. Chem. Soc.* **2007**, *129*, 3828–3829. (f) Ojida, A.; Takashima, I.; Kohira, T.; Nonaka, H.; Hamachi, I. *J. Am. Chem. Soc.* **2008**, *130*, 12095–12101. (g) Shao, N.; Wang, H.; Gao, X.; Yang, R.; Chan, W. *Anal. Chem.* **2010**, *82*, 4628–4636. (h) Chen, W.-H.; Xing, Y.; Pang, Y. *Org. Lett.* **2011**, *13*, 1362–1365.

(21) (a) Vance, D. H.; Czarnik, A. W. *J. Am. Chem. Soc.* **1994**, *116*, 9397–9398. (b) Nishizawa, S.; Kato, Y.; Teramae, N. *J. Am. Chem. Soc.* **1999**, *121*, 9463–9464. (c) Gunnlaugsson, T.; Davis, A. P.; O'Brien, J. E.; Glynn, M. *Org. Lett.* **2002**, *4*, 2449–2452. (d) Aldakov, D.; Anzenbacher, P., Jr. *Chem. Commun.* **2003**, 1394–1395. (e) Gunnlaugsson, T.; Davis, A. P.; O'Brien, J. E.; Glynn, M. *Org. Biomol. Chem.* **2005**, *3*, 48–56. (f) Zyryanov, G. V.; Palacios, M. A.; Anzenbacher, P., Jr. *Angew. Chem., Int. Ed.* **2007**, *46*, 7849–7852. (g) Kim, I.-B.; Han, M. H.; Phillips, R. L.; Samanta, B.; Rotello, V. M.; Zhang, Z. J.; Bunz, U. H. F. *Chem.—Eur. J.* **2009**, *15*, 449–456.

(22) (a) Zhao, X.; Liu, Y.; Schanze, K. S. *Chem. Commun.* **2007**, 2914–2916. (b) Liu, Y.; Schanze, K. S. *Anal. Chem.* **2008**, *80*, 8605–8612. (c) Zhao, X.; Schanze, K. S. *Chem. Commun.* **2010**, *46*, 6075–6077. (d) Wu, C.-Y.; Chen, M.-S.; Lin, C.-A.; Lin, S.-C.; Sun, S.-S. *Chem.—Eur. J.* **2006**, *12*, 2263–2269. (e) Kim, K. M.; Oh, D. J.; Ahn, K. H. *Chem.—Asian J.* **2011**, *6*, 122–127.